Global Change Biology

Optimum growth temperature declines with body size within fish species

Journal:	*Global Change Biology*
Manuscript ID	GCB-21-1622
Wiley - Manuscript type:	Primary Research Articles
Date Submitted by the Author:	05-Aug-2021
Complete List of Authors:	Lindmark, Max; Swedish University of Agricultural Sciences, Department of Aquatic Resources Ohlberger, Jan; University of Washington, School of Aquatic and Fishery Sciences Gårdmark, Anna; Swedish University of Agricultural Sciences, Dept. Aquatic Resources
Keywords:	body growth, metabolic rate, consumption rate, temperature-size rule, metabolic theory of ecology, climate change
Abstract:	According to the temperature-size rule, warming of aquatic ecosystems is generally predicted to increase individual growth rates but reduce asymptotic body sizes of ectotherms. However, we lack a comprehensive understanding of how growth and key processes affecting it, such as consumption and metabolism, depend on both temperature and body mass within species. This limits our ability to inform growth models, link experimental data to observed growth patterns, and advance mechanistic food web models. To examine the combined effects of body size and temperature on individual growth, as well as the link between maximum consumption, metabolism and body growth, we conducted a systematic review and compiled experimental data on fishes from 59 studies that combined body mass and temperature treatments. By fitting hierarchical models accounting for variation between species, we estimated how these three processes scale jointly with temperature and body mass within species. We found that whole-organism maximum consumption increases more slowly with body mass than metabolism, and is unimodal over the full temperature range, which leads to the prediction that optimum growth temperatures decline with body size. Using an independent dataset, we confirmed this negative relationship between optimum growth temperature and size within fish species. Small individuals may therefore exhibit increased growth with initial warming, whereas larger conspecifics could be the first to experience negative impacts of warming on growth. These findings help advance mechanistic models of individual growth and food web dynamics and improve our understanding of how climate warming affects the growth and size structure of aquatic ectotherms.

Title Page

Optimum growth temperature declines with body size within fish species

Max Lindmark[a,1], Jan Ohlberger[b], Anna Gårdmark[c]

[a] Swedish University of Agricultural Sciences, Department of Aquatic Resources, Institute of Coastal Research, Skolgatan 6, Öregrund 742 42, Sweden

[b] School of Aquatic and Fishery Sciences (SAFS), University of Washington, Box 355020, Seattle, WA 98195-5020, USA

[c] Swedish University of Agricultural Sciences, Department of Aquatic Resources, Skolgatan 6, SE-742 42 Öregrund, Sweden

[1] Author to whom correspondence should be addressed. Current address:
Max Lindmark, Swedish University of Agricultural Sciences, Department of Aquatic Resources, Institute of Marine Research, Turistgatan 5, Lysekil 453 30, Sweden, Tel.: +46(0)104784137, **email**: max.lindmark@slu.se

Keywords: body growth, metabolic rate, consumption rate, temperature-size rule, metabolic theory of ecology, climate change

Running head: Optimum growth temperature declines with size

Abstract

According to the temperature-size rule, warming of aquatic ecosystems is generally predicted to increase individual growth rates but reduce asymptotic body sizes of ectotherms. However, we lack a comprehensive understanding of how growth and key processes affecting it, such as consumption and metabolism, depend on both temperature and body mass within species. This limits our ability to inform growth models, link experimental data to observed growth patterns, and advance mechanistic food web models. To examine the combined effects of body size and temperature on individual growth, as well as the link between maximum consumption, metabolism and body growth, we conducted a systematic review and compiled experimental data on fishes from 59 studies that combined body mass and temperature treatments. By fitting hierarchical models accounting for variation between species, we estimated how these three processes scale jointly with temperature and body mass within species. We found that whole-organism maximum consumption increases more slowly with body mass than metabolism, and is unimodal over the full temperature range, which leads to the prediction that optimum growth temperatures decline with body size. Using an independent dataset, we confirmed this negative relationship between optimum growth temperature and size within fish species. Small individuals may therefore exhibit increased growth with initial warming, whereas larger conspecifics could be the first to experience negative impacts of warming on growth. These findings help advance mechanistic models of individual growth and food web dynamics and improve our understanding of how climate warming affects the growth and size structure of aquatic ectotherms.

Introduction

Individual body growth is a fundamental process powered by metabolism, and thus depends on body size and temperature (Brown *et al.* 2004). It affects individual fitness and life history traits, such as maturation size, population growth rates (Savage *et al.* 2004), and ultimately energy transfer across trophic levels (Andersen *et al.* 2009; Barneche & Allen 2018). Therefore, understanding how growth scales with body size and temperature is important for predicting the impacts of global warming on the structure and functioning of ecosystems.

Global warming is predicted to lead to declining body sizes of organisms (Daufresne *et al.* 2009; Gardner *et al.* 2011). The temperature size-rule ('TSR') states that warmer rearing temperatures lead to faster developmental times (and larger initial size-at-age or size-at-life-stage), but smaller adult body sizes in ectotherms (Atkinson 1994; Ohlberger 2013). This relationship is found in numerous experimental studies (Atkinson 1994), is reflected in latitudinal gradients (Horne *et al.* 2015), and is stronger in aquatic than terrestrial organisms (Forster *et al.* 2012; Horne *et al.* 2015). Support for the TSR exists in fishes, in particular in young fish, where reconstructed individual growth histories often reveal positive correlations between growth rates and temperature in natural systems (Thresher *et al.* 2007; Neuheimer *et al.* 2011; Baudron *et al.* 2014; Huss *et al.* 2019). However, whether the positive effect of warming on growth is indeed limited to small individuals within a species, as predicted by the temperature size-rule, is less clear. Negative correlations between maximum size, asymptotic size or size-at-age of old fish and temperature have been found in commercially exploited fish species (Baudron *et al.* 2014; van Rijn *et al.* 2017; Ikpewe *et al.* 2020). However, other studies, including large scale experiments, controlled experiments and latitudinal studies or observational data on unexploited species, have found no or less clear negative relationships between maximum size, growth of old fish or mean size and

temperature (Barneche *et al.* 2019; Huss *et al.* 2019; Van Dorst *et al.* 2019; Audzijonyte *et al.* 2020; Denderen *et al.* 2020) and differences between species may be related to life history traits and depend on local environmental conditions (Denderen *et al.* 2020; Wang *et al.* 2020).

While the support for TSR is mixed, and the underlying mechanisms are not well understood (Ohlberger 2013; Audzijonyte *et al.* 2019; Neubauer & Andersen 2019), theoretical growth models, such as Pütter growth models (Pütter 1920), including the von Bertalanffy growth model (VBGM) (von Bertalanffy 1957), commonly predict declines in asymptotic body mass with temperature and declines in optimum growth temperature with body mass, in line with the TSR (Perrin 1995; Morita *et al.* 2010; Pauly & Cheung 2018b; Pauly 2021). Yet, the physiological basis of these models has been questioned, as the commonly applied scaling parameters (mass exponents) tend to differ from empirical estimates (Lefevre *et al.* 2018; Marshall & White 2019). Hence, despite attempting to describe growth from first principles, Pütter growth models can also be viewed as phenomenological. In more mechanistic growth models, the difference between energy gain and expenditure is partitioned between somatic growth and gonads (Ursin 1967; Kitchell *et al.* 1977; Jobling 1997; Essington *et al.* 2001). Energy gain is normally the amount of energy extracted from consumed food and expenditure, which is defined as maintenance, activity and feeding metabolism. These components of the energetics of growth are found in dynamic energy budget models (Kitchell *et al.* 1977; Kooijman 1993), including those used in physiologically structured population models (PSPMs) (de Roos & Persson 2001) and size-spectrum models (Hartvig *et al.* 2011; Maury & Poggiale 2013; Blanchard *et al.* 2017). Therefore, it is important to understand how consumption and metabolism rates scale with body mass and temperature in order to understand if and how growth of large fish within populations is limited by temperature, and to evaluate the physiological basis of growth models.

Moreover, the effect of body mass and temperature on growth dynamics should be evaluated over ontogeny at the intraspecific level (within species), which better represents the underlying process than interspecific data (among species) (Marshall & White 2019). For instance, we do not expect an interspecific relationship between optimum growth temperature and body mass, but within species it may have a large effect on growth dynamics. Despite this, intraspecific body mass and temperature scaling is often inferred from interspecific data, and we know surprisingly little about average relationship between consumption and metabolic exponents within species (Marshall & White 2019). Importantly, how physiological rates depend on mass and temperature within species can differ from the same relationships across species (Glazier 2005; Rall *et al.* 2012; Jerde *et al.* 2019). Across species, rates are often assumed and found to scale as power functions of mass with exponents of 3/4 for whole organism rates, exponentially with temperature, and with independent mass and temperature effects (e.g., in the Arrhenius fractal supply model (AFS) applied in the metabolic theory of ecology, MTE (Gillooly *et al.* 2001; Brown *et al.* 2004; Downs *et al.* 2008)). In contrast, within species, deviations from a general 3/4 mass exponent are common (Clarke & Johnston 1999; Bokma 2004; Barneche *et al.* 2019; Jerde *et al.* 2019), rates are typically unimodally related to temperature and activation energies can vary a lot (Dell *et al.* 2011; Englund *et al.* 2011; Rall *et al.* 2012; Pawar *et al.* 2016; Uiterwaal & DeLong 2020) and the effects of mass and temperature can be interactive (Xie & Sun 1990; Glazier 2005; García García *et al.* 2011; Ohlberger *et al.* 2012; Lindmark *et al.* 2018) (but see Jerde *et al*. (2019)). Extensions of the MTE include fitting multiple regression models where coefficients for mass and temperature are estimated jointly (Downs *et al.* 2008), as well as fitting non-linear models that can capture the de-activation of biological rates at higher temperatures (Schoolfield *et al.* 1981; Dell *et al.* 2011; Englund *et al.* 2011; Padfield *et al.* 2017). To advance our understanding of the intraspecific

116 properties of mass- and temperature dependence of biological rates, intraspecific data with
117 variation in both mass and temperature are needed.

118 In this study, we analyzed how maximum consumption, metabolism and growth rate of fish
119 scale intraspecifically with mass and temperature. We performed a systematic literature review by
120 searching the Web of Science Core Collection to compile datasets on individual-level maximum
121 consumption, metabolism and growth rates of fish from experiments in which the effect of fish
122 body mass is replicated across multiple temperatures within species (total n=3672, with data from
123 13, 20 and 34 species for each rate, respectively). We then fit hierarchical Bayesian models to
124 estimate general intraspecific scaling parameters while accounting for variation between species.
125 The estimated mass dependence and temperature sensitivity of consumption and metabolism were
126 used to quantify average changes in net energy gain (and hence, growth, assumed proportional to
127 net energy gain) over temperature and body mass. Lastly, we compared our predicted changes in
128 optimum growth temperature over body mass with an independent experimental dataset on
129 optimum growth temperatures across individuals of different sizes within species.
130

131 **Results**

132 We identified that within species of fish, metabolic rates increase faster with body mass than
133 maximum consumption rates, and neither of these rates conform to the commonly predicted 3/4
134 scaling with body mass (Fig. 1). We also quantified the unimodal relationship of consumption rate
135 over the full temperature range (Fig. 2). Combined, these scaling relationships lead to the
136 prediction, based on Pütter-type growth models, that optimum growth temperature declines with
137 body size (Fig. 3). The prediction of declining optimum growth temperatures with size was
138 confirmed by our analysis of independent experimental growth rate data. We find that within

139 species the optimum growth temperature declines with body size by 0.31℃ per unit increase in the
140 natural log of relative body mass (Fig. 4). Below we present the underlying results in more detail.
141 We found that the average intraspecific mass exponent for consumption rate is smaller (0.63
142 [0.55, 0.71]) than that for metabolic rate (0.79 [0.74, 0.84]), based on the non-overlapping
143 Bayesian 95% credible intervals (Fig. 1). It is also probable that the scaling exponents differ from
144 3/4 (that is predicted by the MTE), because >99% of the posterior distribution of the mass exponent
145 of maximum consumption is below 3/4, and 95% of the posterior distribution of the mass exponent
146 of metabolic rate is above 3/4. Activation energies of maximum consumption rate and metabolism
147 are both similar (0.69 [0.54, 0.85] and 0.62 [0.57, 0.67] respectively; Fig. 1) and largely fall within
148 the prediction from the MTE (0.6-0.7 eV) (Brown *et al.* 2004). The global intraspecific intercept
149 for routine and resting metabolic rate is estimated to be 1.85 [1.68, 2.04], and for standard
150 metabolic rate it is 1.29 [0.97, 1.61] (*SI Appendix,* Fig. S7). Models where all coefficients varied
151 by species were favored in terms of WAIC (M5 and M1, for consumption and metabolism,
152 respectively) (*SI Appendix*, Table S4). We found statistical support for a species-varying mass and
153 temperature interaction for metabolic rate; 98% of the posterior distribution of the global
154 interaction coefficient μ_{β_3} is above 0 (*SI Appendix,* Fig. S5). The estimated coefficient is 0.0018
155 [0.015, 0.037] on the Arrhenius temperature scale, which corresponds to a decline in the mass
156 scaling exponent of metabolic rate by 0.0026 $℃^{-1}$. The selected model for maximum consumption
157 rate did not include an interaction term between mass and temperature (M5).
158 We estimated the parameters of the Sharpe-Schoolfield equation (Eq. 4) for temperature-
159 dependence of consumption including data beyond peak temperature as: activation energy, E_j =
160 0.73 [0.54, 0.94], rate at reference temperature, C_{0_j} = 0.79 [0.58, 0.99], temperature at which the
161 rate is reduced to half (of the rate in the absence of deactivation) due to high temperatures, T_h =

0.75 [-0.86, 2.37], and the rate of the decline past the peak, E_h = 1.89 [1.68, 2.1]. This shows that the relationship between consumption rate and temperature is unimodal and asymmetric, where the decline in consumption rate at high temperatures is steeper than the increase at low temperatures (Fig. 2).

The above results provide empirical support for the two criteria outlined in Morita et al., (2010) that result in declining optimum temperatures with size, i.e. (i) smaller whole organism mass exponent for consumption than metabolism (Fig. 1) and (ii) that growth reaches an optimum over temperature. In our case, the second criterion is met because consumption reaches a peak over temperature (Fig. 2) (in contrast to Morita *et al*. (2010), who assumed consumption to be linearly related to temperature, based on data from Atkinson (1994)). We illustrate the consequence of these findings in Fig. 3, which shows that the optimum temperature for net energy gain is reached at a lower temperature for a larger fish because of the difference in mass exponents of consumption and metabolism and because consumption is unimodally related to temperature. Assuming growth is proportional to net energy gain, this predicts that optimum growth temperature declines with body size.

Using independent data from growth trials across a range of body sizes and temperatures, we also find strong statistical support for a decline in optimum growth temperature with body mass within species, because 92% of the posterior density of the global slope estimate ($\mu_{\beta 1}$) is below 0. The models with and without species-varying slopes were indistinguishable in terms of WAIC (*SI Appendix*, Table S5), and we present the results for the species-varying intercept and slope model, due to slightly better model diagnostics (*SI Appendix*, Fig. S24-27). The global relationship is given by the model: $T_{opt} = -0.074 - 0.31 \times m$, where m is the natural log of the rescaled body mass, calculated as the species-specific ratio of mass to maturation mass.

Discussion

In this study, we systematically analyzed the intraspecific scaling of consumption, metabolism and growth with body mass and temperature. We found strong evidence for declining optimum growth temperatures as individuals grow in size, based on two independent approaches. First, we find differences in the intraspecific mass-scaling of consumption and metabolism, and a unimodal temperature dependence of consumption, which lead to predicted declines in optimum temperature for net energy gain (and hence growth) with size. Second, we confirm this prediction using intraspecific growth rate data of fish from temperature experiments. Our analysis thus demonstrates the importance of understanding intraspecific scaling relationships when predicting responses of fish populations to climate warming.

That warming increases growth and development rates but reduces maximum or adult size is well known from experimental studies, also referred to as the temperature-size rule (TSR). Yet, the mechanisms underlying the TSR remain poorly understood. Pütter-type growth models, including the von Bertalanffy growth equation (VBGE), predict that the asymptotic size declines with warming if the ratio of the coefficients for energy gains and losses (H/K in Eq. 7) (Pauly & Cheung 2018b) declines with temperature. However, the assumptions underlying the VBGE were recently questioned because of the lack of empirical basis for the scaling exponents and the effects of those on the predicted effects of temperature on asymptotic size (Lefevre *et al.* 2018; Marshall & White 2019). Specifically, the allometric exponent of energy gains (a) is assumed to be smaller than that of energetic costs (b) (Eq. 7). This is based on the assumption that anabolism scales with the same power as surfaces to volumes ($a = 2/3$) and catabolism, or maintenance metabolism, is proportional to body mass ($b = 1$) (von Bertalanffy 1957; Pauly & Cheung 2018a). In contrast,

maintenance costs are commonly thought to instead be proportional to standard metabolic rate, which in turn often is proportional to intake rates at the interspecific level (Brown *et al.* 2004; Marshall & White 2019). This leads to $a \approx b$, resulting in unrealistic growth trajectories and temperature dependencies of growth dynamics in Pütter models (Lefevre *et al.* 2018; Marshall & White 2019). However, similar to how the existence of large fishes in tropical waters does not invalidate the hypothesis that old individuals of large-bodied fish may reach smaller sizes with warming, interspecific scaling parameters cannot reject or support these model predictions on growth *within* species. We show that the average intraspecific whole-organism mass scaling exponent of metabolism is larger than that of maximum consumption, i.e., the inequality $a < b$ holds at the intraspecific level. By contrast, Pawar *et al.* (2012) estimated larger mass exponents for consumption than metabolic rate (0.84 and 1.04 in 2D and 3D foraging) from interspecific data, which reveals the importance of parameterizing processes occurring over ontogeny with intraspecific rather than interspecific data. When accounting for the smaller intraspecific mass exponent of consumption, and the unimodal thermal response of consumption, the thermal response of net energy gain is characterized by the optimum temperature being a function of body size (Morita *et al.* 2010). Therefore, empirically derived intraspecific parameterizations of simple growth models result in predictions in line with the TSR, in this case via declines in optimum growth temperatures over ontogeny rather than declines in asymptotic sizes.

Declines in optimum growth temperatures over ontogeny as a mechanism for TSR-like growth dynamics do not rely on the assumption that the ratio of the coefficients for energy gains and losses declines with temperature. In fact, we find that when using data from sub-peak temperatures only, the average intraspecific predictions about the activation energy of metabolism and consumption do not differ substantially, which implies there is no clear loss or gain of energetic efficiency with

231 warming within species below temperature optima. This is in contrast to other studies, e.g.
232 Lemoine & Burkepile (2012) and Rall *et al.* (2010). However, it is in line with the finding that
233 growth rates increase with temperature (e.g. Angilletta & Dunham 2003), which is difficult to
234 reconcile from a bioenergetics perspective if warming always reduced net energy gain. Our
235 analysis instead suggests that the mismatch between gains and losses occurs when accounting for
236 unimodal consumption rates over temperature. The match, or mismatch, between the temperature
237 dependence of feeding vs. metabolic rates is a central question in ecology that extends from
238 experiments to meta-analyses to food web models (Vasseur & McCann 2005; Rall *et al.* 2010;
239 Lemoine & Burkepile 2012; Fussmann *et al.* 2014; Lindmark *et al.* 2019). Our study highlights
240 the importance of accounting for non-linear thermal responses for two main reasons. First, the
241 thermal response of net energy gain reaches a peak at temperatures below the peak for
242 consumption. Secondly, as initial warming commonly leads to increased growth rates, the effect
243 of warming on growth rates depends on temperature, and growth should therefore not be assumed
244 to be monotonically related to temperature.

245 Life-stage dependent optimum growth temperatures have previously been suggested as a
246 component of the TSR (Ohlberger 2013). Although previous studies have found declines in
247 optimum growth temperatures with body size in some species of fishes and other aquatic
248 ectotherms (Wyban *et al.* 1995; Panov & McQueen 1998; Steinarsson & Imsland 2003; Björnsson
249 *et al.* 2007; Handeland *et al.* 2008), others have not (Brett *et al.* 1969; Elliott & Hurley 1995).
250 Using systematically collated growth data from experiments with variation in both size and
251 temperature treatments (13 species), we find that for an average fish, the optimum growth
252 temperature declines as it grows in size. This finding emerges despite the small range of body sizes
253 used in the experiments (only 10% of observations are larger than 50% of maturation size) (*SI*

Appendix, Fig. S2). Individuals of such small relative size likely invest little energy in reproduction, which suggests that physiological constraints at warmer temperatures contribute to reduced growth performance of large compared to small fish, in addition to increasing investment into reproduction (Barneche *et al.* 2018).

Translating results from experimental data to natural systems is challenging because maximal feeding rates, unlimited food supply, lack of predation, and constant temperatures do not reflect natural conditions, yet affect growth rates (Brett *et al.* 1969; Lorenzen 1996; Huey & Kingsolver 2019). In addition, total metabolic costs in the wild also include additional costs for foraging and predator avoidance. It is, however, typically found and assumed that standard metabolic rate and natural feeding levels are proportional to routine metabolic rate and maximum consumption rate, respectively, and thus exhibit the same mass-scaling relationships (Kitchell *et al.* 1977; Neuenfeldt *et al.* 2020). Intraspecific growth rates may not appear to be unimodally related to temperature when measured over a temperature gradient across populations within a species (Denderen *et al.* 2020), because each population can be adapted to local climate conditions and thus display different temperature optima. However, each population likely has a thermal optimum for growth, which differs between individuals of different size. Hence, each population might have a unimodal relationship with temperature that differs from other populations of the same species. This highlights the importance of understanding the time scale of environmental change in relation to that of immediate physiological responses, acclimation, adaptation and community reorganization for the specific prediction about climate change impacts. In natural systems, climate warming may also result in stronger food limitation (Ohlberger *et al.* 2011; Huey & Kingsolver 2019). Hence, as optimum growth temperatures decline not only with size but also food availability (Brett *et al.* 1969; Brett 1971), and realized consumption rates are a fraction of the maximum consumption rate

277 (20-70%) (Kitchell *et al.* 1977; Neuenfeldt *et al.* 2019), species may be negatively impacted by
278 warming even when controlled experiments show they can maintain growth capacity at these
279 temperatures. Supporting this point is the observation that warming already has negative or lack
280 of positive effects on body growth in populations living at the edge of their physiological tolerance
281 in terms of growth (Neuheimer *et al.* 2011; Huss *et al.* 2019).

282 Whether the largest fish of a population will be the first to experience negative effects of
283 warming, as suggested by the finding that optimum growth temperature declines with body size,
284 depends on the environmental temperatures they typically experience compared to smaller
285 conspecifics. For instance, large fish may inhabit colder temperatures compared to small fish due
286 to ontogenetic habitat shifts (Werner & Hall 1988; Lloret-Lloret *et al.* 2020); see also Heincke's
287 law (Heincke 1913; Audzijonyte & Pecl 2018). Yet, there is already empirical evidence of the
288 largest individuals in natural populations being the first to suffer from negative impacts of warming
289 from heatwaves (Pörtner & Knust 2007), or not being able to benefit from warming (Huss *et al.*
290 2019; Van Dorst *et al.* 2019). Hence, assuming that warming affects all individuals of a population
291 equally is a simplification that can bias predictions of the biological impacts of climate change.

292 The interspecific scaling of fundamental ecological processes with body mass and temperature
293 has been used to predict the effects of warming on body size, size structure, and population and
294 community dynamics (Vasseur & McCann 2005; Morita *et al.* 2010; Cheung *et al.* 2013; Gilbert
295 *et al.* 2014). We argue that a contributing factor to the discrepancy between mechanistic growth
296 models, general scaling theory, and empirical data has been the lack of data synthesis at the
297 intraspecific level. The approach presented here can help overcome limitations of small data sets
298 by borrowing information across species in a single modelling framework, while accounting for
299 the intraspecific scaling of rates. Accounting for the faster increase in whole-organism metabolism

300 than consumption with body size, the unimodal thermal response of consumption, and resulting
301 size-dependence of optimum growth temperatures is essential for understanding what causes
302 observed growth responses to global warming. Acknowledging these mechanisms is also
303 important for improving predictions on the consequences of warming effects on fish growth for
304 food web functioning, fisheries yields and global food production in warmer climates.
305

306 ## Materials and methods

307 ### Data acquisition

308 We searched the literature for experimental studies evaluating the temperature response of
309 individual maximum consumption rate (feeding rate at unlimited food supply, *ad libitum*), resting,
310 routine and standard oxygen consumption rate as a proxy for metabolic rate (Nelson 2016) and
311 growth rates across individuals of different sizes within species. We used three different searches
312 on the Web of Science Core Collection (see *SI Appendix*, for details). In order to estimate how
313 these rates depend on body size and temperature within species, we selected studies that
314 experimentally varied both body size and temperature (at least two temperature treatments and at
315 least two body masses). The average number of unique temperature treatments (temperature
316 rounded to nearest ℃) by species is 7.2 for growth and 4.3 for consumption and metabolism data.
317 The criteria for both mass and temperature variation in the experiments reduce the number of
318 potential data sets, as most experimental studies use either size or temperature treatments, not both.
319 However, these criteria allow us to fit multiple regression models and estimate the effects of mass
320 and temperature jointly, and to evaluate the probability of interactive mass- and temperature effects
321 within species. Following common practice we excluded larval studies, which represents a life

322 stage exhibiting different constraints and scaling relationships than non-larval life stages (Glazier
323 2005).

324 Studies were included if (i) a unique experimental temperature was recorded for each trial (± 1°
325 C), (ii) fish were provided food at *ad libitum* (consumption and growth data) or if they were unfed
326 (resting, standard or routine metabolic rate), and (iii) fish exhibited normal behavior during the
327 experiments. We used only one study per species and rate to ensure that all data within a given
328 species are comparable as measurements of these rates can vary between studies due to e.g.
329 measurement bias, differences in experimental protocols, or because different populations were
330 studied (Armstrong & Hawkins 2008; Jerde *et al.* 2019). In cases where we found more than one
331 study for a given rate and species, we selected the most suitable study based on our pre-defined
332 criteria (for details, see *SI Appendix*). We ensured that the experiments were conducted at
333 ecologically relevant temperatures (*SI Appendix,* Figs. S1, S3). A more detailed description of the
334 search protocol, data selection, acquisition, quality control, collation of additional information and
335 standardizing of rates to common units can be found in *SI Appendix*.

336 We compiled four datasets: maximum consumption rate, metabolic rate, growth rate and the
337 optimum growth temperature for each combination of body mass group and species. We compiled
338 a total of 746 measurements of maximum consumption rate (of which 666 are below peak), 2699
339 measurements of metabolic rate and 227 measurements of growth rate (45 optimum temperatures)
340 from published articles for each rate, from 20, 34 and 13 species, respectively, from different
341 taxonomic groups, habitats and lifestyles (Table S1-S2). We requested original data from all
342 corresponding authors of each article. In cases where we did not hear from the corresponding
343 author, we extracted data from tables or figures using Web Plot Digitizer (Rohatgi 2012).
344

345 **Model fitting**

346 *Model description*

347 To each dataset, we fit hierarchical models with different combinations of species-varying
348 coefficients, meaning they are estimated with shrinkage. This reduces the influence of outliers
349 which could occur in species with small samples sizes (Gelman & Hill 2007; Harrison *et al.* 2018).
350 The general form of the model is:

351 $$y_{ij} \sim N(\mu_{ij}, \sigma) \quad (1)$$

352 $$\mu_{ij} = \beta_{0j} + \sum_{p=1}^{n} (\beta_p \times x_{ip}) \quad (2)$$

353 $$\beta_{0j} \sim N(\mu_{\beta_0}, \sigma_{\beta_0}) \quad (3)$$

354 where y_{ij} is the ith observation for species j for rate y, β_{0j} is a species-varying intercept, x_{ip} is a
355 predictor and β_p is its coefficient, with $p = 1,..n$, where n is the number of predictors considered
356 in the model (mass, temperature, and their interaction). Predictors are mean centered to improve
357 interpretability (Schielzeth 2010). Species-level intercepts follow a normal distribution with
358 hyperparameters μ_{β_0} (global intercept) and σ_{β_0} (between-species standard deviation). For most
359 models we also allow the coefficient β_p to vary between species, such that β_p becomes β_{pj} and x_{ip}
360 x_{ijp}, where $\beta_{pj} \sim N(\mu_{\beta_p}, \sigma_{\beta_p})$. For each dataset, we evaluate multiple combinations of species-
361 varying coefficients (from varying intercept to n varying coefficients). We used a mix of flat,
362 weakly informative, and non-informative priors. For the temperature and mass coefficients we
363 used the predictions from the MTE as the means of the normal prior distributions (Brown *et al.*
364 2004), but with large standard deviations (see *SI Appendix*, Table S3). Below we describe how the
365 model in Eqns. 1-3 is applied to each data set.

366

Mass- and temperature dependence of consumption, metabolism and growth below peak temperatures

Peak temperature (optimum in the case of growth) refers to the temperature at which the rate was maximized, by size group. For data below peak temperatures, we assumed that maximum consumption rate, metabolism and growth scale allometrically (as a power function of the form $I = i_0 M^{b_0}$) with mass, and exponentially with temperature. Hence, after log-log (natural log) transformation of mass and the rate, and temperature in Arrhenius temperature ($1/kT$ in unit eV^{-1}, where k is Boltzmann's constant [8.62×10^{-5} eV K^{-1}]), the relationship between the rate and its predictors becomes linear. This is similar to the MTE, except that we estimate all coefficients instead of correcting rates, and allow not only the intercepts but also slopes to vary across species.

When applied to Eqns. 1-3, y_{ij} is the ith observation for species j of the natural log of the rate (consumption, metabolism or growth), and the predictors are m_{ij} (natural log of body mass), $t_{A,ij}$ (Arrhenius temperature, $1/kT$ in unit eV^{-1}), both of which were mean-centered, and their interaction. Body mass is in g, consumption rate in g day^{-1}, metabolic rate in mg $\mathrm{O_2}$ h^{-1} and specific growth rate in unit % day^{-1}. We use resting or routine metabolism (mean oxygen uptake of a resting unfed fish only showing some spontaneous activity) and standard metabolism (resting unfed and no activity, usually inferred from extrapolation or from low quantiles of routine metabolism, e.g. lowest 10% of measurements) to represent metabolic rate (Beamish 1964; Ohlberger *et al.* 2007). Routine and resting metabolism constitute 58% of the data used and standard metabolism constitutes 42%. We accounted for potential differences between these types of metabolic rate measurements by adding two dummy coded variables, $type_r$ and $type_s$, the former taking the value 0 for standard and 1 for a routine or resting metabolic rate measurement, and vice versa for the latter variable. Thus, for metabolism, we replace the overall intercept β_{0j} in

Eqns. 2-3 with β_{0rj} and β_{0sj}. β_{0sj} is forced to 0 for a species that has a routine or resting metabolic rate and β_{0rj} is forced to 0 for a species with standard metabolic rate data. We assume these coefficients vary by species following normal distributions with global means $\mu_{\beta_{0r}}$ and $\mu_{\beta_{0s}}$, and standard deviations $\sigma_{\beta_{0r}}$ and $\sigma_{\beta_{0s}}$, i.e. $\beta_{0rj} \sim N(\mu_{\beta_{0r}}, \sigma_{\beta_{0r}})$ and $\beta_{0sj} \sim N(\mu_{\beta_{0s}}, \sigma_{\beta_{0s}})$.

Mass- and temperature dependence of consumption including beyond peak temperatures

Over a large temperature range, many biological rates are unimodal. We identified such tendencies in 10 out of 20 species in the consumption data set. To characterize the decline in consumption rate beyond peak temperature, we fit a mixed-effects version of the Sharpe Schoolfield equation (Schoolfield *et al.* 1981) as expressed in (Padfield *et al.* 2020), to equations 1-2 with y_{ij} as rescaled consumption rates (C). Specifically, we model μ_{ij} in Eq. 1 with the Sharpe-Schoolfield equation:

$$\mu_{ij} = \frac{C_{0_j}(T_c) e^{E_j\left(\frac{1}{kT_C} - \frac{1}{kT}\right)}}{1 + e^{E_h\left(\frac{1}{kT_h} - \frac{1}{kT}\right)}} \quad (4)$$

$$E_j \sim N(\mu_E, \sigma_E) \quad (5)$$

$$C_{0_j} \sim N(\mu_{C_0}, \sigma_{C_0}) \quad (6)$$

where $C_{0_j}(T_C)$ is the rate at a reference temperature T_C in Kelvin [K] (here set to 263.15), E_j [eV] is the activation energy, E_h [eV] characterizes the decline in the rate past the peak temperature and T_h [K] is the temperature at which the rate is reduced to half (of the rate in the absence of deactivation) due to high temperatures. We assume E_j and C_{0_j} vary across species according to a normal distribution with means μ_E and μ_{C_0}, and standard deviations σ_E and σ_{C_0} (Eq. 5-6). Prior to rescaling maximum consumption (in unit g day $^{-1}$) by dividing $C_{i,j}$ with the mean within species $\overline{C_j}$, we isolate the effect of mass by dividing consumption with $m^{0.63}$, which is the estimated

allometric relationship from the log-linear model. Temperature, T, is centered by subtracting the temperature at peak consumption. This was estimated separately for each species using the Sharpe-Schoolfield equation but without group-varying coefficients in a frequentist framework (see '*Parameter estimation*'). The rescaling is done to control for differences in the optimum temperature between species, which if not accounted for obscures the average relationship between consumption and temperature among species.

Mass-dependence of optimum growth temperature

To evaluate how the optimum temperature ($t_{opt,ij}$, in degrees Celsius) for individual growth depends on body mass, we fit Eqns. 1-3 with y_{ij} as the mean-centered optimum growth temperature within species ($t_{opt,ij} = T_{opt,ij} - \overline{T}_{opt,j}$), to account for species being adapted to different thermal regimes. m_{ij}, the predictor variable for this model, is the natural log of the ratio between mass and mass at maturation acquired from FishBase (Froese & Pauly 2019), within species: $m_{ij} = \ln(M_{ij}/M_{mat,j}) - \overline{\ln(M_{ij}/M_{mat,j})}$. This rescaling is done because we are interested in examining relationships within species over "ontogenetic size", and because we do not expect an interspecific relationship between optimum growth temperature and body mass because species are adapted to different thermal regimes. We consider both the intercept and the effect of mass to potentially vary between species.

Parameter estimation

We fit the models in a Bayesian framework, using R version 4.0.2 (R Core Team 2020) and JAGS (Plummer 2003) through the R-package '*rjags*' (Plummer 2019). We used 3 Markov chains with 5000 iterations for adaptation, followed by 15000 iterations burn-in and 15000 iterations sampling

where every 5th iteration saved. Model convergence was assessed by visually inspecting trace plots and potential scale reduction factors ($\hat{R}$) (*SI Appendix*). $\hat{R}$ compares chain variance with the pooled variance, and values <1.1 suggest all three chains converged to a common distribution (Gelman *et al.* 2003). We relied heavily on the R packages within '*tidyverse'* (Wickham *et al.* 2019) for data processing, as well as '*ggmcmc*' (Fernández-i-Marín 2016), '*mcmcviz*' (Youngflesh 2018) and '*bayesplot*' (Gabry *et al.* 2019) for visualization. Single-species Sharpe-Schoolfield models were fitted using the packages '*rTPC'* (Padfield & O'Sullivan 2020) and '*nls.multstart'* (Padfield & Matheson 2020)

Model comparison

We compared the parsimony of models with different hierarchical structures, and with or without mass-temperature interactions, using the Watanabe-Akaike information criterion (WAIC) (Watanabe 2013; Vehtari *et al.* 2017), which is based on the posterior predictive distribution. We report WAIC for each model descried above (Table S4-S5), and examine models with ΔWAIC values < 2, where ΔWAIC is each models difference to the lowest WAIC across models, in line with other studies (Olmos *et al.* 2019).

Net energy gain

The effect of temperature and mass dependence of maximum consumption and metabolism (proportional to biomass gain and losses, respectively) (Ursin 1967; Kitchell *et al.* 1977; Essington *et al.* 2001) on growth is illustrated by visualizing the net energy gain. The model for the net energy gain (growth) can be viewed as an empirical temperature-dependent Pütter-type model. Pütter-type models are the simplest growth models based on a dynamic energy budget, and make strong

assumptions about mass-scaling of key life-history and physiological processes (e.g., maturation and assimilation). However, Pütter-type models are among the most commonly applied growth models in ecology and fisheries, they tend to fit data reasonably well (Marshall & White 2019), and are suitable for illustrating the consequences of non-linear consumption rates due to their simplicity (in contrast to more complex and parameter-rich dynamic energy budget models, e.g. (Kitchell *et al.* 1977; Cuenco *et al.* 1985)). A Pütter model is the result of two antagonistic allometric processes, biomass gains and biomass losses:

$$\frac{dM}{dt} = H(T)M^a - K(T)M^b \quad (7)$$

where M is body mass and T is temperature, H and K the allometric constants and a and b the exponents of the processes underlying gains and losses, respectively. We convert metabolism from oxygen consumption [mg O_2 h^{-1} day^{-1}] to g day^{-1} by assuming 1 kcal = 295 mg O_2 (based on an oxycaloric coefficient of 14.2 J/mg O_2) (Hepher 1988), 1 kcal = 4184 J and an energy content of 5600 J/g (wet weight) (Rijnsdorp & Ibelings 1989). Consumption rate is already in unit g day^{-1}. Consumption and metabolic rates are calculated for two sizes (5 and 1000 g, which roughly correspond to the 25th percentile of both datasets and the maximum mass in the consumption data, respectively), using the global allometric relationships found in the log-log models fit to sub-peak temperatures. These allometric functions are further scaled with the temperature correction factors r_c for consumption and r_m for metabolism. r_c is based on the Sharpe-Schoolfield model and r_m is given by the temperature dependence of metabolic rate from the log-linear model. Because r_c and r_m are fitted to data on different scales, we divide these functions by their maximum. Lastly, we rescale the product between the allometric functions and r_c and r_m such that the rate at 19°C (mean temperature in both data sets) equals the temperature-independent rate.

Acknowledgements

We thank Hiroki Yamanaka, Dennis Tomalá Solano, Vanessa Messmer, Björn Björnsson, Albert Imsland, Tomas Árnasson, Yiping Luo, Takeshi Tomiyama and Myron Peck for generously providing data; Magnus Huss and Ken Haste Andersen, for providing useful comments on earlier versions of the manuscript; Daniel Padfield and Wilco Verberk for helpful discussions; Matthew Low and Malin Aronsson for an introduction to Bayesian inference. This study was supported by grants from the Swedish Research Council FORMAS (no. 217-2013-1315) and the Swedish Research Council (no. 2015-03752) (both to AG).

Author contributions

ML conceived the study; ML, JO, AG designed research; ML performed research with input from JO and AG; ML, JO, AG wrote the paper and contributed to revisions of the manuscript.

Data accessibility statement

All data and R code (lists of studies in literature search, data preparation, analyses and figures) can be downloaded from a GitHub repository (https://github.com/maxlindmark/scaling) and will be archived on Zenodo upon publication.

References

Andersen, K.H., Beyer, J.E. & Lundberg, P. (2009). Trophic and individual efficiencies of size-structured communities. *Proceedings of the Royal Society B: Biological Sciences*, 276, 109–114.

Angilletta, M.J. & Dunham, A.E. (2003). The temperature-size rule in ectotherms: simple evolutionary explanations may not be general. *The American Naturalist*, 162, 332–342.

Armstrong, J.D. & Hawkins, L.A. (2008). Standard metabolic rate of pike, *Esox lucius*: variation among studies and implications for energy flow modelling. *Hydrobiologia*, 601, 83–90.

Atkinson, D. (1994). Temperature and organism size—A biological law for ectotherms? In: *Advances in Ecological Research*. Elsevier, pp. 1–58.

Audzijonyte, A., Barneche, D.R., Baudron, A.R., Belmaker, J., Clark, T.D., Marshall, C.T., *et al.* (2019). Is oxygen limitation in warming waters a valid mechanism to explain decreased body sizes in aquatic ectotherms? *Global Ecology and Biogeography*, 28, 64–77.

Audzijonyte, A. & Pecl, G.T. (2018). Deep impact of fisheries. *Nature Ecology & Evolution*, 2, 1348–1349.

Audzijonyte, A., Richards, S.A., Stuart-Smith, R.D., Pecl, G., Edgar, G.J., Barrett, N.S., *et al.* (2020). Fish body sizes change with temperature but not all species shrink with warming. *Nat Ecol Evol*, 4, 809–814.

Barneche, D.R. & Allen, A.P. (2018). The energetics of fish growth and how it constrains food-web trophic structure. *Ecology Letters*, 21, 836–844.

Barneche, D.R., Jahn, M. & Seebacher, F. (2019). Warming increases the cost of growth in a model vertebrate. *Functional Ecology*, 33, 1256–1266.

Barneche, D.R., Robertson, D.R., White, C.R. & Marshall, D.J. (2018). Fish reproductive-energy output increases disproportionately with body size. *Science*, 360, 642–645.

Baudron, A.R., Needle, C.L., Rijnsdorp, A.D. & Marshall, C.T. (2014). Warming temperatures and smaller body sizes: synchronous changes in growth of North Sea fishes. *Global Change Biology*, 20, 1023–1031.

Beamish, F.W.H. (1964). Respiration of fishes with special emphasis on standard oxygen consumption II. Influence of weight and temperature on respiration of several species'. *Canadian Journal of Zoology/Revue Canadienne de Zoologie*, 42, 177–188.

von Bertalanffy, L. (1957). Laws in metabolism and growth. *The quarterly review of biology*, 32, 217–231.

Björnsson, B., Steinarsson, A. & Árnason, T. (2007). Growth model for Atlantic cod (*Gadus morhua*): Effects of temperature and body weight on growth rate. *Aquaculture*, 271, 216–226.

Blanchard, J.L., Heneghan, R.F., Everett, J.D., Trebilco, R. & Richardson, A.J. (2017). From bacteria towWhales: Using functional size spectra to model marine ecosystems. *Trends in Ecology & Evolution*, 32, 174–186.

Bokma, F. (2004). Evidence against universal metabolic allometry. *Functional Ecology*, 18, 184–187.

Brett, J.R. (1971). Energetic responses of salmon to temperature. A study of some thermal relations in the physiology and freshwater ecology of sockeye salmon (*Oncorhynchus nerka*). *Integr Comp Biol*, 11, 99–113.

Brett, J.R., Shelbourn, J.E. & Shoop, C.T. (1969). Growth rate and body composition of fingerling sockeye salmon, *Oncorhynchus nerka*, in relation to temperature and ration size. *J. Fish. Res. Bd. Can.*, 26, 2363–2394.

Brown, J.H., Gillooly, J.F., Allen, A.P., Savage, V.M. & West, G.B. (2004). Toward a metabolic theory of ecology. *Ecology*, 85, 1771–1789.

Cheung, W.W.L., Sarmiento, J.L., Dunne, J., Frölicher, T.L., Lam, V.W.Y., Deng Palomares, M.L., *et al.* (2013). Shrinking of fishes exacerbates impacts of global ocean changes on marine ecosystems. *Nature Climate Change*, 3, 254–258.

Clarke, A. & Johnston, N.M. (1999). Scaling of metabolic rate with body mass and temperature in teleost fish. *Journal of Animal Ecology*, 68, 893–905.

Cuenco, M.L., Stickney, R.R. & Grant, W.E. (1985). Fish bioenergetics and growth in aquaculture ponds: I. Individual fish model development. *Ecological Modelling*, 27, 169–190.

Daufresne, M., Lengfellner, K. & Sommer, U. (2009). Global warming benefits the small in aquatic ecosystems. *Proceedings of the National Academy of Sciences, USA*, 106, 12788–12793.

Dell, A.I., Pawar, S. & Savage, V.M. (2011). Systematic variation in the temperature dependence of physiological and ecological traits. *Proceedings of the National Academy of Sciences*, 108, 10591–10596.

Denderen, D. van, Gislason, H., Heuvel, J. van den & Andersen, K.H. (2020). Global analysis of fish growth rates shows weaker responses to temperature than metabolic predictions. *Global Ecology and Biogeography*, 29, 2203–2213.

Downs, C.J., Hayes, J.P. & Tracy, C.R. (2008). Scaling metabolic rate with body mass and inverse body temperature: A test of the Arrhenius fractal supply model. *Functional Ecology*, 22, 239–244.

Elliott, J.M. & Hurley, M.A. (1995). The functional relationship between body size and growth rate in fish. *Functional Ecology*, 9, 625.

Englund, G., Öhlund, G., Hein, C.L. & Diehl, S. (2011). Temperature dependence of the functional response. *Ecology Letters*, 14, 914–921.

Essington, T.E., Kitchell, J.F. & Walters, C.J. (2001). The von Bertalanffy growth function, bioenergetics, and the consumption rates of fish. *Canadian Journal of Fisheries and Aquatic Sciences*, 58, 2129–2138.

Fernández-i-Marín, X. (2016). ggmcmc: Analysis of MCMC Samples and Bayesian Inference. *Journal of Statistical Software*, 70, 1–20.

Forster, J., Hirst, A.G. & Atkinson, D. (2012). Warming-induced reductions in body size are greater in aquatic than terrestrial species. *PNAS*, 109, 19310–19314.

Froese, R. & Pauly, D. (2019). *Editors. FishBase*. World Wide Web electronic publication. www.fishbase.org, (12/2019).

Fussmann, K.E., Schwarzmüller, F., Brose, U., Jousset, A. & Rall, B.C. (2014). Ecological stability in response to warming. *Nature Climate Change*, 4, 206–210.

Gabry, J., Simpson, D., Vehtari, A., Betancourt, M. & Gelman, A. (2019). Visualization in Bayesian workflow. *J. R. Stat. Soc. A*, 182, 389–402.

García García, B., Cerezo Valverde, J., Aguado-Giménez, F., García García, J. & Hernández, M.D. (2011). Effect of the interaction between body weight and temperature on growth and maximum daily food intake in sharpsnout sea bream (*Diplodus puntazzo*). *Aquaculture International*, 19, 131–141.

Gardner, J.L., Peters, A., Kearney, M.R., Joseph, L. & Heinsohn, R. (2011). Declining body size: a third universal response to warming? *Trends in Ecology & Evolution*, 26, 285–291.

Gelman, A., Carlin, J., Stern, H. & Rubin, D. (2003). *Bayesian Data Analysis. 2nd edition*. Chapman and Hall/CRC, Boca Raton.

Gelman, A. & Hill, J. (2007). *Data Analysis Using Regression and Multilevel/Hierarchical Models*. Cambridge University Press.

Gilbert, B., Tunney, T.D., McCann, K.S., DeLong, J.P., Vasseur, D.A., Savage, V.M., *et al.* (2014). A bioenergetic framework for the temperature dependence of trophic interactions. *Ecology Letters*, 17, 902–914.

596 Gillooly, J.F., Brown, J.H., West, G.B., Savage, V.M. & Charnov, E.L. (2001). Effects of size
597 and temperature on metabolic rate. *Science*, 2248-2251.
598 Glazier, D.S. (2005). Beyond the "3/4-power law": variation in the intra- and interspecific
599 scaling of metabolic rate in animals. *Biological Reviews of the Cambridge Philosophical*
600 *Society*, 80, 611–662.
601 Handeland, S.O., Imsland, A.K. & Stefansson, S.O. (2008). The effect of temperature and fish
602 size on growth, feed intake, food conversion efficiency and stomach evacuation rate of
603 Atlantic salmon post-smolts. *Aquaculture*, 283, 36–42.
604 Harrison, X.A., Donaldson, L., Correa-Cano, M.E., Evans, J., Fisher, D.N., Goodwin, C.E.D., *et*
605 *al.* (2018). A brief introduction to mixed effects modelling and multi-model inference in
606 ecology. *PeerJ*, 6, e4794.
607 Hartvig, M., Andersen, K.H. & Beyer, J.E. (2011). Food web framework for size-structured
608 populations. *Journal of Theoretical Biology*, 272, 113–122.
609 Heincke, F. (1913). Rapp. Proc. Verb. Réun. ICES 16, 1–70.
610 Hepher, B. (1988). *Nutrition of Pond Fishes*. Cambridge University Press.
611 Horne, C.R., Hirst, Andrew.G. & Atkinson, D. (2015). Temperature-size responses match
612 latitudinal-size clines in arthropods, revealing critical differences between aquatic and
613 terrestrial species. *Ecology Letters*, 18, 327–335.
614 Huey, R.B. & Kingsolver, J.G. (2019). Climate warming, resource availability, and the metabolic
615 meltdown of ectotherms. *The American Naturalist*, 194, E140–E150.
616 Huss, M., Lindmark, M., Jacobson, P., Van Dorst, R.M. & Gårdmark, A. (2019). Experimental
617 evidence of gradual size-dependent shifts in body size and growth of fish in response to
618 warming. *Glob Change Biol*, 25, 2285–2295.
619 Ikpewe, I.E., Baudron, A.R., Ponchon, A. & Fernandes, P.G. (2020). Bigger juveniles and
620 smaller adults: Changes in fish size correlate with warming seas. *Journal of Applied*
621 *Ecology*, Early View.
622 Jerde, C.L., Kraskura, K., Eliason, E.J., Csik, S.R., Stier, A.C. & Taper, M.L. (2019). Strong
623 Evidence for an Intraspecific Metabolic Scaling Coefficient Near 0.89 in Fish. *Front.*
624 *Physiol.*, 10, 1166.
625 Jobling, M. (1997). Temperature and growth: modulation of growth rate via temperature change.
626 In: *Global Warming: Implications for Freshwater and Marine Fish* (eds. Wood, C.M. &
627 McDonald, D.G.). Cambridge University Press, Cambridge, pp. 225–254.
628 Kitchell, J.F., Stewart, D.J. & Weininger, D. (1977). Applications of a bioenergetics model to
629 yellow perch (*Perca flavescens*) and walleye (*Stizostedion vitreum vitreum*). *Journal of*
630 *the Fisheries Board of Canada*, 34, 1922–1935.
631 Kooijman, S.A.L.M. (1993). *Dynamic energy budgets in biological systems*. Cambridge
632 University Press.
633 Lefevre, S., McKenzie, D.J. & Nilsson, G.E. (2018). In modelling effects of global warming,
634 invalid assumptions lead to unrealistic projections. *Global Change Biology*, 24, 553–556.
635 Lemoine, N.P. & Burkepile, D.E. (2012). Temperature-induced mismatches between
636 consumption and metabolism reduce consumer fitness. *Ecology*, 93, 2483–2489.
637 Lindmark, M., Huss, M., Ohlberger, J. & Gårdmark, A. (2018). Temperature-dependent body
638 size effects determine population responses to climate warming. *Ecology Letters*, 21,
639 181–189.
640 Lindmark, M., Ohlberger, J., Huss, M. & Gårdmark, A. (2019). Size-based ecological
641 interactions drive food web responses to climate warming. *Ecology Letters*, 22, 778–786.

642 Lloret-Lloret, E., Navarro, J., Giménez, J., López, N., Albo-Puigserver, M., Pennino, M.G., *et al.*
643 (2020). The seasonal distribution of a highly commercial fish is related to ontogenetic
644 changes in its feeding strategy. *Front. Mar. Sci.*, 7.
645 Lorenzen, K. (1996). The relationship between body weight and natural mortality in juvenile and
646 adult fish: a comparison of natural ecosystems and aquaculture. *Journal of Fish Biology*,
647 49, 627–642.
648 Marshall, D.J. & White, C.R. (2019). Have we outgrown the existing models of growth? *Trends*
649 *in Ecology & Evolution*, 34, 102–111.
650 Maury, O. & Poggiale, J.-C. (2013). From individuals to populations to communities: A dynamic
651 energy budget model of marine ecosystem size-spectrum including life history diversity.
652 *Journal of Theoretical Biology*, 324, 52–71.
653 Morita, K., Fukuwaka, M., Tanimata, N. & Yamamura, O. (2010). Size-dependent thermal
654 preferences in a pelagic fish. *Oikos*, 119, 1265–1272.
655 Nelson, J.A. (2016). Oxygen consumption rate v. rate of energy utilization of fishes: a
656 comparison and brief history of the two measurements. *Journal of Fish Biology*, 88, 10–
657 25.
658 Neubauer, P. & Andersen, K.H. (2019). Thermal performance of fish is explained by an interplay
659 between physiology, behaviour and ecology. *Conserv Physiol*, 7.
660 Neuenfeldt, S., Bartolino, V., Orio, A., Andersen, K.H., Andersen, N.G., Niiranen, S., *et al.*
661 (2020). Feeding and growth of Atlantic cod (*Gadus morhua* L.) in the eastern Baltic Sea
662 under environmental change. *ICES Journal of Marine Science*, 77, 624–632.
663 Neuheimer, A.B., Thresher, R.E., Lyle, J.M. & Semmens, J.M. (2011). Tolerance limit for fish
664 growth exceeded by warming waters. *Nature Climate Change*, 1, 110–113.
665 Ohlberger, J. (2013). Climate warming and ectotherm body size – from individual physiology to
666 community ecology. *Functional Ecology*, 27, 991–1001.
667 Ohlberger, J., Edeline, E., Vollestad, L.A., Stenseth, N.C. & Claessen, D. (2011). Temperature-
668 driven regime shifts in the dynamics of size-structured populations. *The American*
669 *Naturalist*, 177, 211–223.
670 Ohlberger, J., Mehner, Thomas., Staaks, Georg. & Hölker, Franz. (2012). Intraspecific
671 temperature dependence of the scaling of metabolic rate with body mass in fishes and its
672 ecological implications. *Oikos*, 121, 245–251.
673 Ohlberger, J., Staaks, G. & Hölker, F. (2007). Effects of temperature, swimming speed and body
674 mass on standard and active metabolic rate in vendace (*Coregonus albula*). *Journal of*
675 *Comparative Physiology, B*, 177, 905–916.
676 Olmos, M., Payne, M.R., Nevoux, M., Prévost, E., Chaput, G., Pontavice, H.D., *et al.* (2019).
677 Spatial synchrony in the response of a long range migratory species (*Salmo salar*) to
678 climate change in the North Atlantic Ocean. *Global Change Biology*, 26, 1319–1337.
679 Padfield, D., Castledine, M. & Buckling, A. (2020). Temperature-dependent changes to host–
680 parasite interactions alter the thermal performance of a bacterial host. *The ISME Journal*,
681 14, 389–398.
682 Padfield, D., Lowe, C., Buckling, A., Ffrench-Constant, R., Jennings, S., Shelley, F., *et al.*
683 (2017). Metabolic compensation constrains the temperature dependence of gross primary
684 production. *Ecology Letters*, 20, 1250–1260.
685 Padfield, D. & Matheson, G. (2020). *nls.multstart: Robust Non-Linear regression using AIC*
686 *Scores*.
687 Padfield, D. & O'Sullivan, H. (2020). *rTPC: Functions for fitting thermal performance curves*.

688 Panov, V.E. & McQueen, D.J. (1998). Effects of temperature on individual growth rate and body
689 size of a freshwater amphipod, 76, 1107–1116.
690 Pauly, D. (2021). The gill-oxygen limitation theory (GOLT) and its critics. *Science Advances*, 7,
691 eabc6050.
692 Pauly, D. & Cheung, W.W.L. (2018a). On confusing cause and effect in the oxygen limitation of
693 fish. *Global Change Biology*, 24, e743–e744.
694 Pauly, D. & Cheung, W.W.L. (2018b). Sound physiological knowledge and principles in
695 modeling shrinking of fishes under climate change. *Global Change Biology*, 24, e15–e26.
696 Pawar, S., Dell, A.I., Savage, V.M. & Knies, J.L. (2016). Real versus Artificial Variation in the
697 Thermal Sensitivity of Biological Traits. *The American Naturalist*, 187, E41–E52.
698 Pawar, S., Dell, A.I., & Van M. Savage. (2012). Dimensionality of consumer search space drives
699 trophic interaction strengths. *Nature*, 486, 485–489.
700 Perrin, N. (1995). About Berrigan and Charnov's life-history puzzle. *Oikos*, 137–139.
701 Plummer, M. (2003). JAGS: A program for analysis of Bayesian graphical models using Gibbs
702 sampling. *Working Papers*, 8.
703 Plummer, M. (2019). *rjags*.
704 Pörtner, H.O. & Knust, R. (2007). Climate change affects marine fishes through the oxygen
705 limitation of thermal tolerance. *Science*, 315, 95–97.
706 Pütter, A. (1920). Studien über physiologische Ähnlichkeit VI. Wachstumsähnlichkeiten.
707 *Pflügers Arch.*, 180, 298–340.
708 R Core Team. (2020). *R: A Language and Environment for Statistical Computing. R Foundation*
709 *for Statistical Computing*. Vienna, Austria.
710 Rall, B.C., Brose, U., Hartvig, M., Kalinkat, G., Schwarzmuller, F., Vucic-Pestic, O., *et al.*
711 (2012). Universal temperature and body-mass scaling of feeding rates. *Philosophical*
712 *Transactions of the Royal Society of London, Series B: Biological Sciences*, 367, 2923–
713 2934.
714 Rall, B.C., Vucic-Pestic, O., Ehnes, R.B., Emmerson, M. & Brose, U. (2010). Temperature,
715 predator–prey interaction strength and population stability. *Global Change Biology*, 16,
716 2145–2157.
717 van Rijn, I., Buba, Y., DeLong, J., Kiflawi, M. & Belmaker, J. (2017). Large but uneven
718 reduction in fish size across species in relation to changing sea temperatures. *Global*
719 *Change Biology*, 23, 3667–3674.
720 Rijnsdorp, A.D. & Ibelings, B. (1989). Sexual dimorphism in the energetics of reproduction and
721 growth of North Sea plaice, Pleuronectes platessa L. *Journal of Fish Biology*, 35, 401–
722 415.
723 Rohatgi, A. (2012). *WebPlotDigitalizer: HTML5 based online tool to extract numerical data*
724 *from plot images. Version 4.1. [WWW document] URL*
725 *https://automeris.io/WebPlotDigitizer (accessed on January 2019).*
726 de Roos, A.M. & Persson, L. (2001). Physiologically structured models – from versatile
727 technique to ecological theory. *Oikos*, 94, 51–71.
728 Savage, V.M., Gillooly, J.F., Brown, J.H., West, G.B. & Charnov, E.L. (2004). Effects of body
729 size and temperature on population growth. *The American Naturalist*, 163, 429–441.
730 Schielzeth, H. (2010). Simple means to improve the interpretability of regression coefficients:
731 Interpretation of regression coefficients. *Methods in Ecology and Evolution*, 1, 103–113.

Schoolfield, R.M., Sharpe, P.J.H. & Magnuson, C.E. (1981). Non-linear regression of biological temperature-dependent rate models based on absolute reaction-rate theory. *Journal of Theoretical Biology*, 88, 719–731.

Steinarsson, A. & Imsland, A.K. (2003). Size dependent variation in optimum growth temperature of red abalone (*Haliotis rufescens*). *Aquaculture*, 224, 353–362.

Thresher, R.E., Koslow, J.A., Morison, A.K. & Smith, D.C. (2007). Depth-mediated reversal of the effects of climate change on long-term growth rates of exploited marine fish. *Proceedings of the National Academy of Sciences, USA*, 104, 7461–7465.

Uiterwaal, S.F. & DeLong, J.P. (2020). Functional responses are maximized at intermediate temperatures. *Ecology*, 101, e02975.

Ursin, E. (1967). A Mathematical Model of Some Aspects of Fish Growth, Respiration, and Mortality. *Journal of the Fisheries Research Board of Canada*, 24, 2355–2453.

Van Dorst, R.M., Gårdmark, A., Svanbäck, R., Beier, U., Weyhenmeyer, G.A. & Huss, M. (2019). Warmer and browner waters decrease fish biomass production. *Global Change Biology*, 25, 1395–1408.

Vasseur, D.A. & McCann, K.S. (2005). A mechanistic approach for modelling temperature-dependent consumer-resource dynamics. *The American Naturalist*, 166, 184–198.

Vehtari, A., Gelman, A. & Gabry, J. (2017). Practical Bayesian model evaluation using leave-one-out cross-validation and WAIC. *Stat Comput*, 27, 1413–1432.

Wang, H.-Y., Shen, S.-F., Chen, Y.-S., Kiang, Y.-K. & Heino, M. (2020). Life histories determine divergent population trends for fishes under climate warming. *Nature Communications*, 11, 4088.

Watanabe, S. (2013). A Widely Applicable Bayesian Information Criterion. *Journal of Machine Learning Research*, 14, 867–897.

Werner, E.E. & Hall, D.J. (1988). Ontogenetic habitat shifts in bluegill: The foraging rate-predation risk trade-off. *Ecology*, 69, 1352–1366.

Wickham, H., Averick, M., Bryan, J., Chang, W., D'Agostino McGowan, L., François, R., *et al.* (2019). Welcome to the tidyverse. *Journal of Open Source Software*, 1686.

Wyban, J., Walsh, W.A. & Godin, D.M. (1995). Temperature effects on growth, feeding rate and feed conversion of the Pacific white shrimp (*Penaeus vannamei*). *Aquaculture*, 138, 267–279.

Xie, Xiaojun. & Sun, Ruyung. (1990). The Bioenergetics of the Southern Catfish (*Silurus meridionalis* Chen). I. Resting Metabolic Rate as a Function of Body Weight and Temperature. *Physiological Zoology*, 63, 1181–1195.

Youngflesh, C. (2018). MCMCvis: Tools to Visualize, Manipulate, and Summarize MCMC Output. *Journal of Open Source Software*, 3, 640.

769 **Figures**

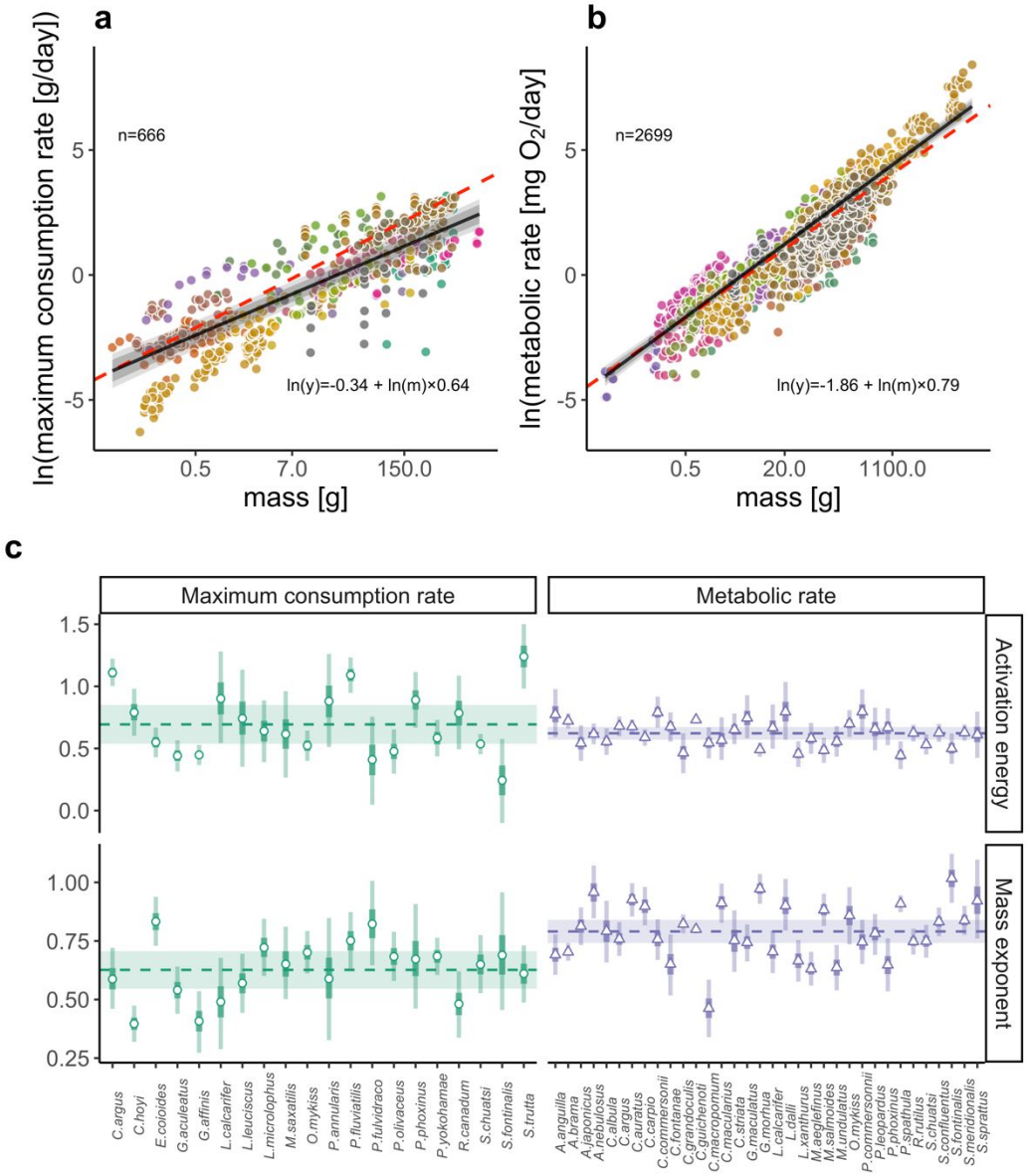

770

771 **Figure 1.** *Natural log of maximum consumption rate (A) and metabolic rate (B) against body mass*
772 *on a logarithmic x-axis. Lines are global predictions (routine metabolic rate in panel B) at the*
773 *average temperature in each data set (both 19*℃*, but note the model is fitted using mean-centred*
774 *Arrhenius temperature), hence the temperature terms are omitted. Red dahsed lines indicate a*
775 *slope of 3/4, corresponding to the prediction from the metabolic theory of ecology. Shaded areas*
776 *correspond to 80% and 95% credible intervals. Species are grouped by color (legend not shown,*

n=20 for consumption and n=34 for metabolism, respectively). C) Global and species-level effects of mass and temperature on maximum consumption rate and metabolic rate. Horizontal lines show the posterior medians of the global activation energies and mass exponents of maximum consumption and metabolism (μ_{β_1} and μ_{β_2} in Eqs. 6-8 for the mass and temperature coefficients, respectively). The shaded horizontal rectangles correspond to the posterior median ± 2 standard deviations. Points and triangles show the posterior medians for each species-level coefficient (for maximum consumption rate and metabolic rate, respectively), and the vertical bars show their 80% and 95% credible interval.

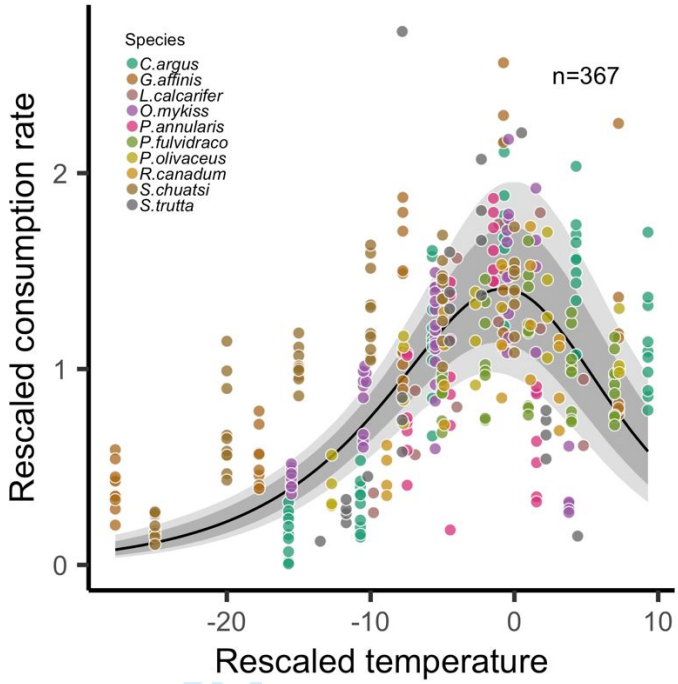

Figure 2. *Mass-corrected maximum consumption rate increases until a maximum is reached, after which it declines steeper than the initial rate of increase. Maximum consumption rates are relative to the average maximum consumption rates within species and temperature is the difference between the experimental temperature and the temperature where maximum consumption peaks (also by species). Lines show posterior median of predictions from the Sharpe-Schoolfield model (using the average intercept across species and the common coefficients), grey bands show 95% and 80% credible intervals. Colors indicate species.*

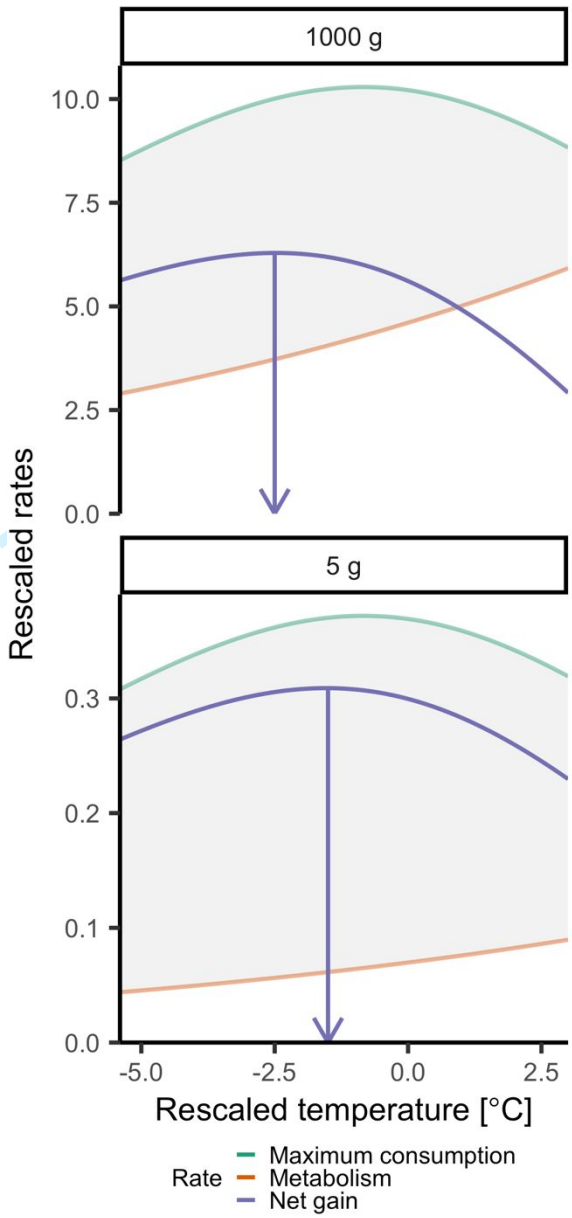

Figure 3. *Illustration of predicted whole-organism maximum consumption rate (green), metabolic rate (purple) and the difference between them (orange) for two body sizes (top=1000g, bottom=5g) (see ´Materials and Methods´). Vertical arrows indicate the temperature where the difference in net energy gain (energy available for growth) is maximized for the two body sizes, which occurs at different temperatures despite that consumption peaks at the same temperature for both body sizes.*

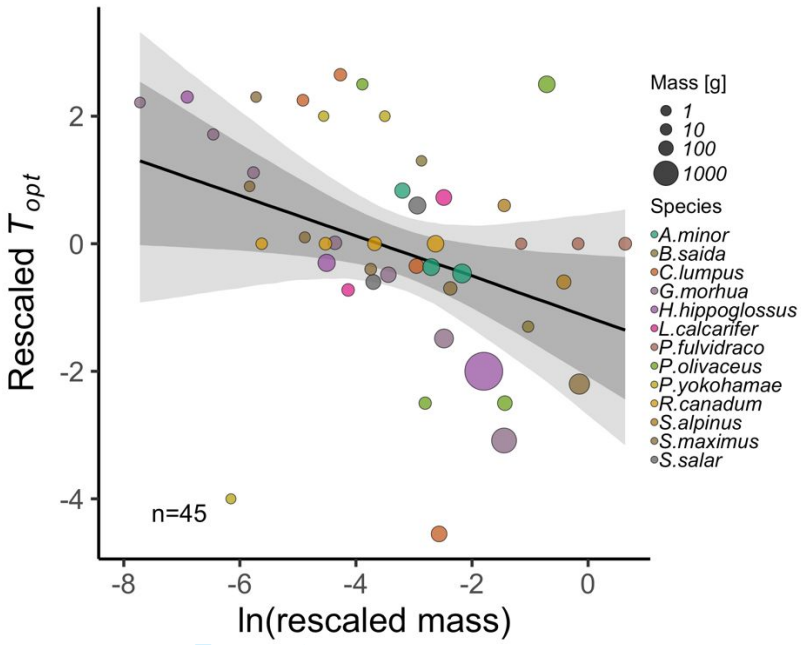

804

805 **Figure 4.** *Experimental data demonstrating optimum growth temperature declines with*
806 *intraspecific body mass. The plot shows the optimum temperature within species (rescaled by*
807 *subtracting the mean optimum temperature from each observation, by species) as a function of the*
808 *natural log of rescaled body mass (ratio of mass to maturation mass within species). Probability*
809 *bands represent 80% and 95% credible intervals, and the solid line shows the global prediction (*
810 μ_{β_0} *and* μ_{β_1}*). Colors indicate species and the area of the circle corresponds to body mass in unit*
811 g.

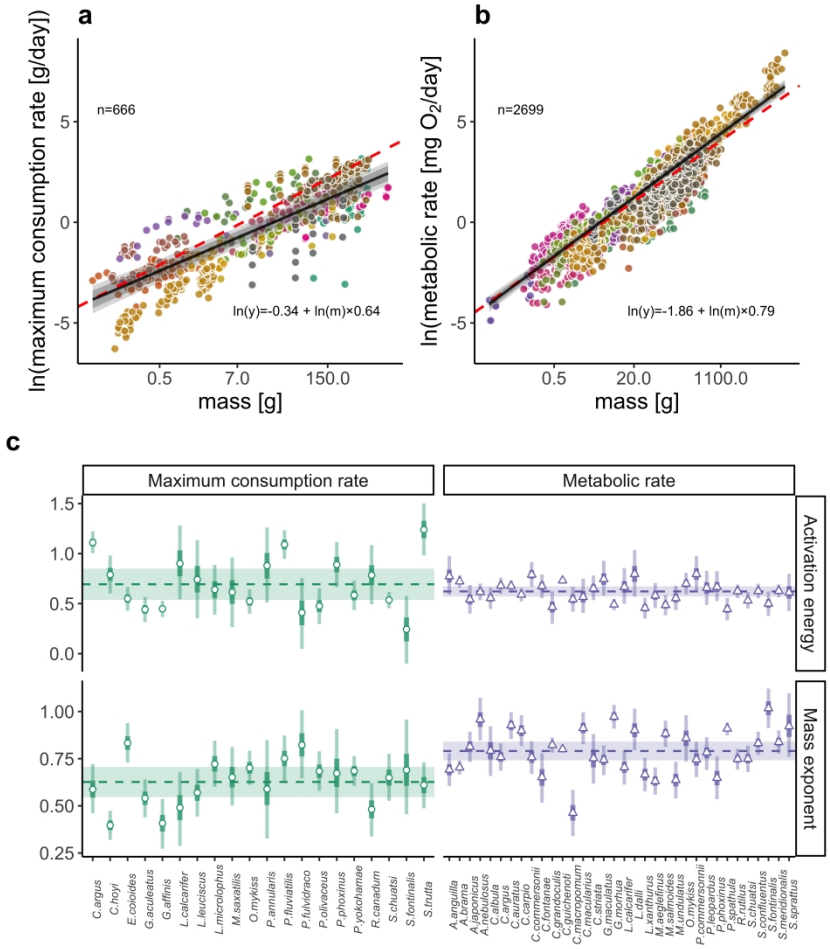

Natural log of maximum consumption rate (A) and metabolic rate (B) against body mass on a logarithmic x-axis. Lines are global predictions (routine metabolic rate in panel B) at the average temperature in each data set (both 19℃, but note the model is fitted using mean-centred Arrhenius temperature), hence the temperature terms are omitted. Red dahsed lines indicate a slope of 3/4, corresponding to the prediction from the metabolic theory of ecology. Shaded areas correspond to 80% and 95% credible intervals. Species are grouped by color (legend not shown, n=20 for consumption and n=34 for metabolism, respectively). C) Global and species-level effects of mass and temperature on maximum consumption rate and metabolic rate. Horizontal lines show the posterior medians of the global activation energies and mass exponents of maximum consumption and metabolism ($\mu_{\beta 1}$ and $\mu_{\beta 2}$ in Eqs. 6-8 for the mass and temperature coefficients, respectively). The shaded horizontal rectangles correspond to the posterior median ± 2 standard deviations. Points and triangles show the posterior medians for each species-level coefficient (for maximum consumption rate and metabolic rate, respectively), and the vertical bars show their 80% and 95% credible interval.

1833x1833mm (72 x 72 DPI)

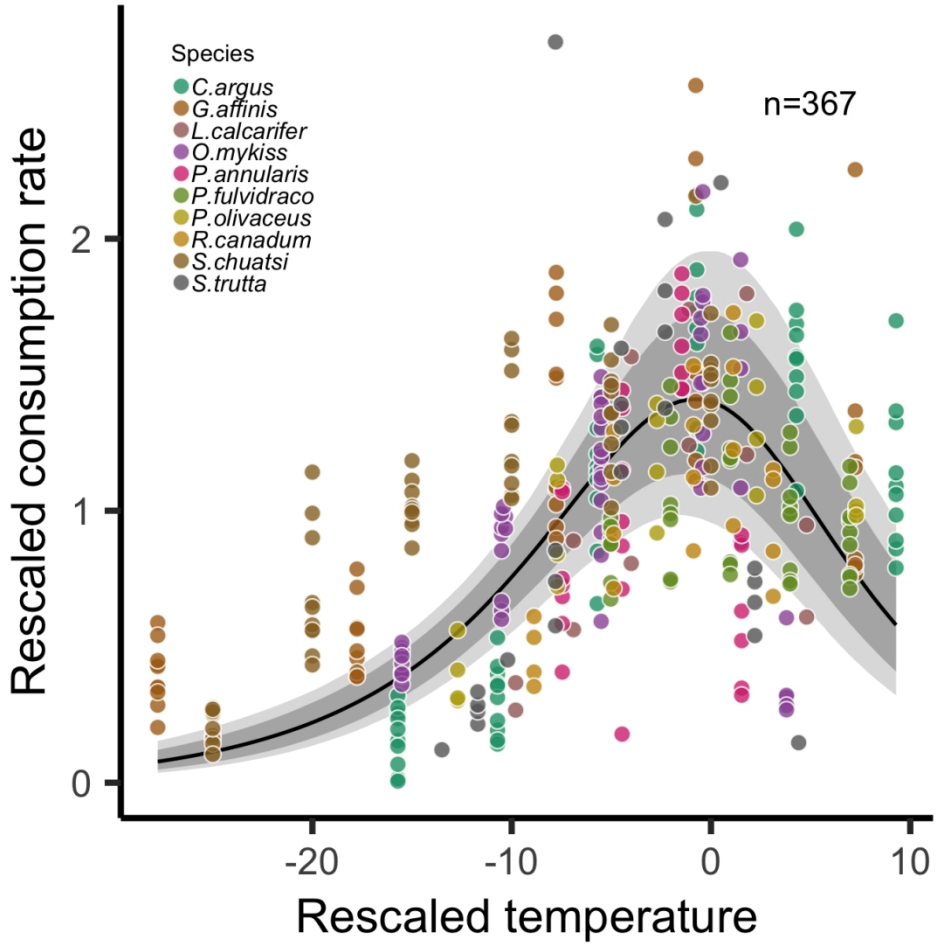

Figure 2. Mass-corrected maximum consumption rate increases until a maximum is reached, after which it declines steeper than the initial rate of increase. Maximum consumption rates are relative to the average maximum consumption rates within species and temperature is the difference between the experimental temperature and the temperature where maximum consumption peaks (also by species). Lines show posterior median of predictions from the Sharpe-Schoolfield model (using the average intercept across species and the common coefficients), grey bands show 95% and 80% credible intervals. Colors indicate species.

499x499mm (72 x 72 DPI)

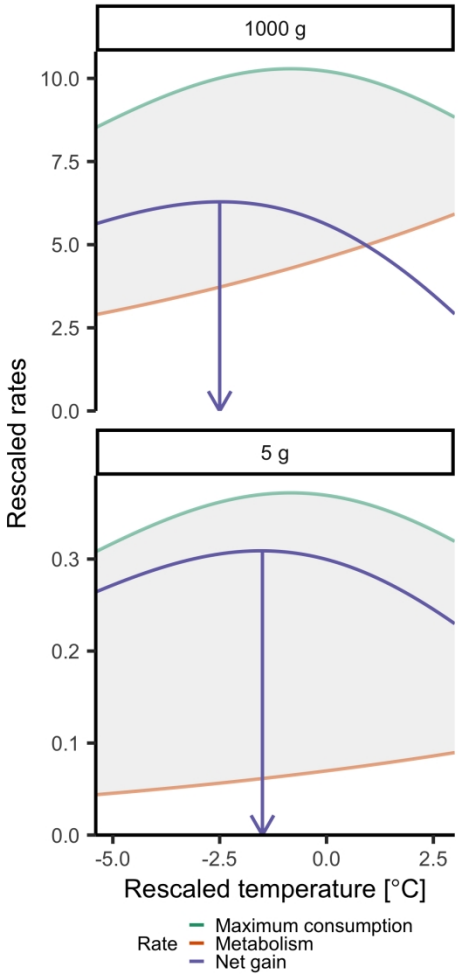

Illustration of predicted whole-organism maximum consumption rate (green), metabolic rate (purple) and the difference between them (orange) for two body sizes (top=1000g, bottom=5g) (see ´Materials and Methods´). Vertical arrows indicate the temperature where the difference in net energy gain (energy available for growth) is maximized for the two body sizes, which occurs at different temperatures despite that consumption peaks at the same temperature for both body sizes.

916x916mm (72 x 72 DPI)

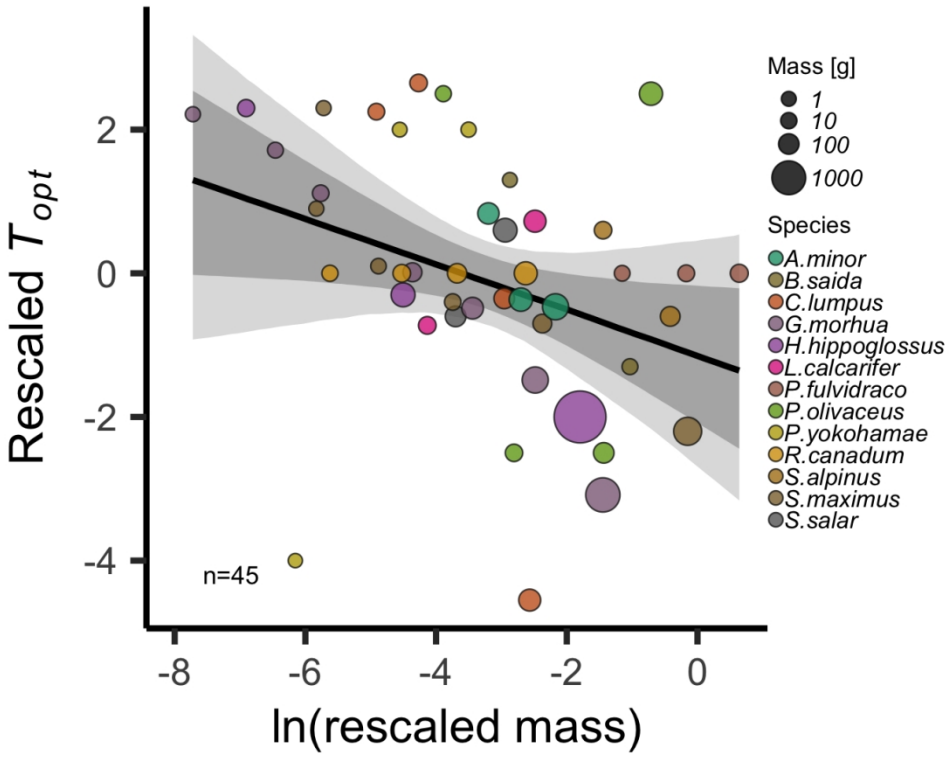

Figure 4. Experimental data demonstrating optimum growth temperature declines with intraspecific body mass. The plot shows the optimum temperature within species (rescaled by subtracting the mean optimum temperature from each observation, by species) as a function of the natural log of rescaled body mass (ratio of mass to maturation mass within species). Probability bands represent 80% and 95% credible intervals, and the solid line shows the global prediction ($\mu_{\beta 0}$ and $\mu_{\beta 1}$). Colors indicate species and the area of the circle corresponds to body mass in unit g.

499x499mm (72 x 72 DPI)